DOI: 10.1002/ejic.200900902

Syntheses, Crystal Structures and Gas Sorption Properties of Prussian Blue Analogues Constructed from $[Cr(CN)_6]^{3-}$ Building Blocks

Ai-Hua Yuan,*[a] Chao-Xia Chu,[a] Hu Zhou,[a] Peng Yuan,[b] Kang-Kang Liu,[a] Li Li,[a] Qing-Feng Zhang,[a] Xin Chen,[a] and Yi-Zhi Li[c]

Keywords: Microporous materials / Prussian blue analogues / Structure elucidation / Adsorption

Three isostructural porous Prussian blue analogues $KM[Cr(CN)_6]\cdot H_2O$ (M = Zn, Mn, Fe) with alkali metal cations K^+ located within the pores of the frameworks have been constructed and characterized structurally. Thermal gravimetric analysis and variable-temperature powder XRD results indicate that the three porous materials are stable at high temperatures, and their frameworks are still retained after dehydration. The permanent porosities have been confirmed by nitrogen and hydrogen sorption measurements at 77 K. Sorption studies show that the framework of FeCr with just 289 $m^2 g^{-1}$ BET surface area can take up a moderate amount of H_2 at 77 K and 860 Torr [112 cm^3(STP) g^{-1}, 0.71 wt.-%], which indicates that the guest alkali metal cation K^+ located in the pores can enhance the H_2 binding affinity within the dehydrated porous framework.

Introduction

The US Department of Energy (DOE) has set the performance targets for onboard hydrogen storage systems to have densities of 6.0 wt.-% and 45 g L^{-1} [at ambient temperature (from 40 to 95 °C) and applicable pressure (less than 100 atm)] by 2010 and 9.0 wt.-% and 81 g L^{-1} by 2015.[1] Following these goals, several families of porous materials have been evaluated in the past decades to increase the hydrogen storage density in porous solids, such as, carbon-based solids,[2] zeolites[3] and metal–organic frameworks.[4]

More recently, cyanometallate-based materials have attracted escalating research interest, because in comparison to traditional zeolites, they possess lower framework densities, higher surface areas and lower enthalpies of adsorption, which have led to an enormous application potential in gas storage.[5,6] To enhance hydrogen uptake capacities of these porous materials, particularly at near ambient temperature, great efforts have been devoted to the exploration of various strategies to increase hydrogen affinities of porous frameworks. Among them, the implementation of coordinatively unsaturated metal centres into porous frameworks has been considered one of the most attractive ways. As a result, several types of cyanide-based porous solids with open transition-metal sites located at the surfaces of the channels and/or cavities have been evaluated for hydrogen storage.[6] The most promising materials are the dehydrated Prussian blue analogues of the type $M_3[Co(CN)_6]_2$ (M = Mn, Fe, Co, Ni, Cu, Zn, Cd),[6i,6j,7] which contain open M^{2+} coordination sites as a result of vacancies at $[Co(CN)_6]^{3-}$ sites within the cubic framework. Amongst them, $Cu_3[Co(CN)_6]_2$ exhibits the highest H_2 storage capacity, taking up 1.8 wt.-% at 77 K and 890 Torr. In particular, the family of compounds $A_2Zn_3[Fe(CN)_6]_2\cdot xH_2O$ (A = H, Li, Na, K, Rb, Cs), provided an opportunity for studying the strength of H_2 interactions with the exchangeable alkali metal cations located within the cavities of an anionic metal–cyanide framework.[6d,6e,8] Upon dehydration, a maximum excess uptake of 1.2 wt.-% at 77 K and 1.2 bar and a maximum isosteric heat of adsorption of 9.0 kJ mol^{-1} were observed for $K_2Zn_3[Fe(CN)_6]_2$.

We report here the syntheses, crystal structures and nitrogen and hydrogen sorption properties of a family of porous Prussian blue analogues $KM[Cr(CN)_6]\cdot H_2O$ (M = Zn, Mn, Fe) (labelled as $MCr\cdot H_2O$ in the following), where the framework metal coordination environment remains saturated with atoms from the CN bridges but with the exposed alkali metal cation K^+. To our surprise, gas sorption properties of the cyanometallate-based porous materials based on the $[Cr(CN)_6]^{3-}$ building block remain poorly documented to date,[5c,5f] and H_2 sorption have not yet been reported.

[a] School of Material Science and Engineering, Jiangsu University of Science and Technology,
Zhenjiang 212003, China
Fax: +86-511-84448290
E-mail: aihuayuan@163.com
[b] Guangzhou Institute of Geochemistry, Chinese Academy of Sciences,
Guangzhou 510640, China
[c] Coordination Chemistry Institute and the State Key Laboratory of Coordination Chemistry, Nanjing University,
Nanjing 210093, China

Supporting information for this article is available on the WWW under http://dx.doi.org/10.1002/ejic.200900902.

Results and Discussion

Crystal Structures of $MCr{\cdot}H_2O$ (M = Zn, Mn, Fe)

Single-crystal X-ray diffraction analysis revealed that the three Prussian blue analogues $MCr{\cdot}H_2O$ (M = Mn, Zn, Fe) were isostructural with each other, crystallizing in space group $Fm\bar{3}n$. The formula determined from single-crystal structural data is in agreement with the composition based on elemental and ICP analysis results.

The crystal structures of $MCr{\cdot}H_2O$ are closely related to those of the polymers reported previously.[9] Selected bond lengths for $MCr{\cdot}H_2O$ are gathered in Table 1. Octahedral $[Cr(CN)_6]^{3-}$ units are linked via octahedrally coordinated, nitrogen-bound M^{2+} ions to give a cubic porous framework, as shown in Figure 1. The cavities of the cubic lattice are occupied by guest H_2O molecules, and the alkali metal K^+ cations play the role in charge balance, with K and O atoms fixed to have 50% occupancy each. Calculations within PLATON[10] by using the VOID routine revealed that about 36% of the unit cell was void and thus large free space for guest molecules sorption. These water molecules can be removed upon heating, leaving the $KM[Cr(CN)_6]$ framework intact and generating open coordination sites on the alkali metal cation K^+.

Table 1. Bond lengths [Å] for $MCr{\cdot}H_2O$.

Compound	$ZnCr{\cdot}H_2O$	$MnCr{\cdot}H_2O$	$FeCr{\cdot}H_2O$
M1–N1	2.072(5)	2.174(4)	1.975(6)
Cr1–C1	2.031(6)	2.066(5)	2.020(6)
C1–N1	1.187(8)	1.157(6)	1.277(10)

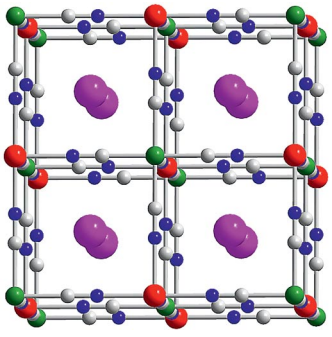

Figure 1. Porous framework for the cubic phases $MCr{\cdot}H_2O$. Red, green, grey and blue spheres represent M, Cr, C and N atoms, respectively. The cavities are occupied by K^+ ions and guest H_2O molecules (pink spheres).

Thermal Stabilities and Structural Integrities of $MCr{\cdot}xH_2O$

TGA and powder XRD were used to evaluate the thermal stabilities and structural integrities of $MCr{\cdot}xH_2O$. For as-synthesized fresh samples of $MCr{\cdot}xH_2O$ (M = Zn, Mn), room-temperature powder XRD (Figure 2) results revealed the same pattern of intense diffraction lines in each of the simulated and as-synthesized materials. However, significantly decreased diffraction intensities and broadened deflections have been observed for $FeCr{\cdot}xH_2O$, which is thought to be associated with the fact that Fe^{II} hexacyanochromate(III) is an unstable coordination compound, which on aging partially transforms into metal hexacyanoferrate(II) to form a more stable solid. In addition, the IR absorption band observed at about 2085 cm^{-1} (Figure S3, Supporting Information) also corresponds to the presence of metal–N–C–Fe^{II}–C–N–metal chains in the sample, which indicates partial decomposition of the sample. However, this decomposition is not distinguished by variable-temperature powder XRD and cannot lead to a loss in porosity, as detailed below. Efforts to control the synthesized process to improve the shape of peaks were unsuccessful.

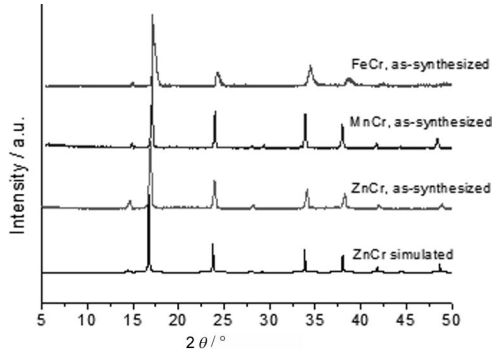

Figure 2. Powder XRD patterns of the as-synthesized MCr powders compared to those simulated from single-crystal XRD data of ZnCr.

As shown in Figure 3, as-synthesized $MCr{\cdot}xH_2O$ lost the crystal water molecules completely below ca. 100 °C, and then the dehydrated structures remained stable, preserving their porous feature, up to ca. 330, 250 and 220 °C for ZnCr, MnCr and FeCr, respectively. The hydration degree is estimated from the weight loss and these compounds contain a large amount of water molecules, from 5.8 to 7.8 molecules per formula unit depending on the metal involved.

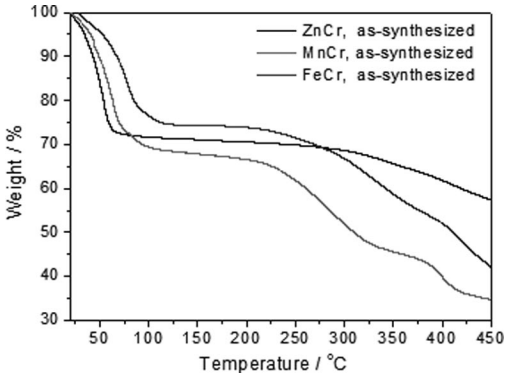

Figure 3. Thermogravimetric curves of $MCr{\cdot}xH_2O$.

Furthermore, the porous frameworks of $MCr{\cdot}xH_2O$ were largely intact when the guest molecules were removed by soft heating, and the structure of the dehydrated phase re-

mained at higher temperatures, as evidenced by comparison of the variable-temperature powder XRD patterns (Figure 4; Figure S4 and S5, Supporting Information) collected at temperatures ranging from room temperature to 270 °C (Figure 4). A slight weight loss from 200 to 270 °C for MnCr (M = Mn, Fe) can be attributed to the partial decomposition of the sample, which cannot lead to the complete collapse of the framework. It should be noted that the powder XRD pattern after dehydration in the region 10–50°/2θ of MnCr matched well with that of a related complex,[9] which indicated that both complexes have the same crystal structure.

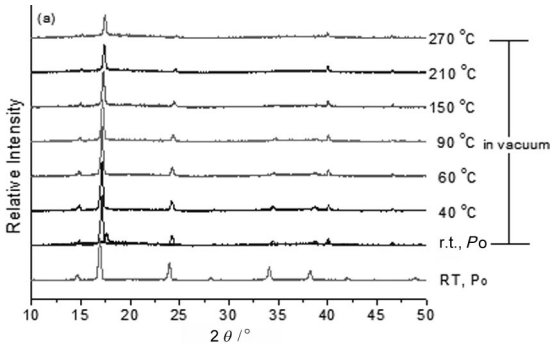

Figure 4. Variable-temperature powder XRD patterns of as-synthesized ZnCr.

It is noticeable that upon removal of water the unit cell contracted, as was observed between the hydrated and dehydrated phases. An analogue structural effect on dehydration has been reported for other porous cyanometallates upon dehydration.[5j,11] In particular, about 4.4% contraction of the unit cell parameter refined by using FullProf Rietveld software[12] was observed for the dehydrated ZnCr framework (Figure 5) heated from 40 to 390 °C under vacuum. The cell contraction was detected from an obvious peak shift to higher values in the variable-temperature powder XRD patterns.

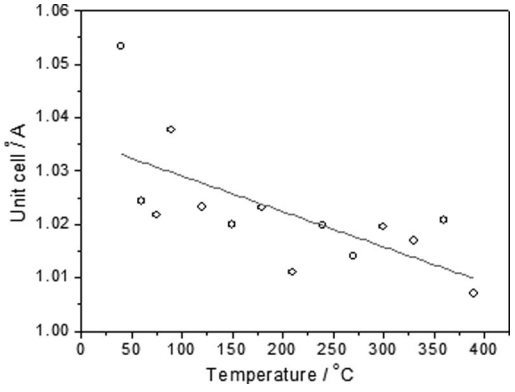

Figure 5. Temperature-dependent unit cell of ZnCr·xH$_2$O from variable-temperature powder XRD data obtained under vacuum conditions.

N_2 Adsorption Measurements of MCr (M = Zn, Mn, Fe)

The colours of the MCr series changed after dehydration, and during the dehydration process, the colour of as-synthesized ZnCr changed from light-yellow to orange-red, MnCr changed from light-green to orange-red and FeCr changed from brick red to dark red. However, these colour changes are not necessarily indicative of a loss of structure, which was evidenced by IR spectra analysis (Figures S1–S3, Supporting Information).

To investigate the permanent porosities of the three materials, nitrogen sorption isotherms were measured at 77 K for freshly prepared samples that were completely dehydrated by heating at 120 °C for 12 h under vacuum. As shown in Figure 6, all of them showed reversible type I sorption behaviour, as expected for microporous materials. Respective N_2 uptakes of 226, 181 and 112 cm^3(STP) g^{-1} (Table 2) are observed that correspond to 3.3, 2.6 and 1.6 N_2 molecules per formula unit, respectively (assuming only negligible reductions in the unit cell dimensions as a result of dehydration).

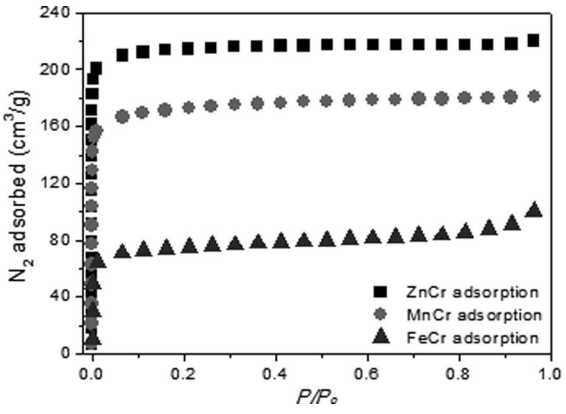

Figure 6. Nitrogen adsorption isotherms for the dehydrated MCr Prussian blue analogues.

Table 2. Nitrogen and hydrogen sorption properties of the dehydrated MCr phases.

	SA[a] [m^2 g^{-1}]	N_2[b] uptake [cm^3(STP) g^{-1}]	H_2[c] uptake [cm^3(STP) g^{-1}]	H_2[c] [wt.-%]	H_2[d] [wt.-%]
ZnCr	869	226	138	1.22	1.66
MnCr	688	181	97	0.86	1.25
FeCr	289	112	81	0.71	1.00

[a] BET plots were constructed for nitrogen sorption isotherms, and nominal surface areas were determined by using a linear section over the range P/P_0 = 0.001–0.03. [b] Measured at 77 K and 0.99 P/P_0. [c] Measured at 77 K and 860 Torr. [d] Predicted through application of the Langmuir–Freundlich equation.

Fittings of the Brunauer–Emmett–Teller (BET) equation to the adsorption isotherms of nitrogen give the estimated surface areas of 869, 688 and 289 m^2 g^{-1} for ZnCr, MnCr and FeCr, respectively (Table 2), compared to 560–870 m^2 g^{-1} for Prussian blue analogues $M_3[Co(CN)_6]_2$ (M = Mn. Fe, Cu, Ni, Cu, Zn)[6i] and 220–518 m^2 g^{-1} for the porous tetracyanometallates.[5e,5h] Using the Dubinin–Radushkevich (DR) equation,[13] the respective pore volumes were estimated to be 0.32, 0.25, and 0.10 cm^3 g^{-1}, respectively.

The significantly lower surface area and N_2 uptake observed for FeCr is likely attributed to the partial sample decomposition within crystallites as above discussed. Similar phenomena have also been observed in related cyanometallates[5h,6e,6i] and in the metal–organic framework $[Cu_2(bptc)(H_2O)_2(dmf)_3(H_2O)]$.[14] Significantly, owing to the presence of the K^+ guest cation in the framework structure of MCr, the surface areas observed are generally lower than the reported values for related dehydrated $M_3[Co(CN)_6]_2$ Prussian blue analogues.[6i]

H_2 Sorption Measurements of MCr (M = Zn, Mn, Fe)

To evaluate hydrogen storage performance, hydrogen sorption isotherms were measured at 77 K. As shown in Figure 7, all three compounds revealed reversible type Ib isotherms without any hysteresis, indicative of permanent porosity. To the best of our knowledge, these are the first hydrogen sorption measurements reported for any Prussian blue analogues based on the $[Cr(CN)_6]^{3-}$ building block.

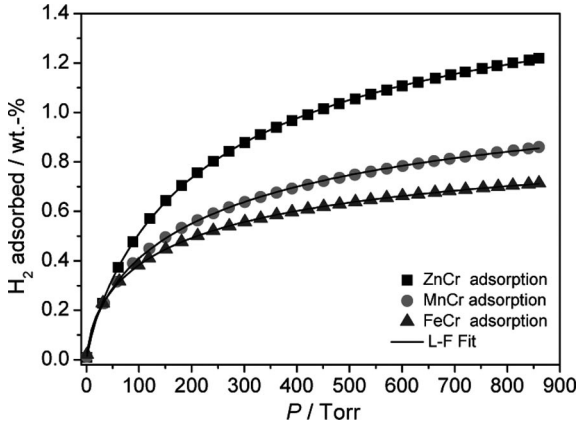

Figure 7. Hydrogen adsorption isotherms for the dehydrated MCr Prussian blue analogues in gravimetric unit (wt.-%). Solid lines represent the best fits of the Langmuir–Freundlich (L-F) equation to the data.

Uptake at 77 K and 860 Torr varies from 0.71 wt.-% (excess) in FeCr to a maximum of 1.22 wt.-% H_2 in ZnCr. This trend in hydrogen adsorption is consistent with BET surface areas extracted from nitrogen adsorption data, but it must be remembered that saturation of the surfaces by hydrogen is not accomplished at this pressure. Note that the value observed for ZnCr is slightly below the 1.5 wt.-% of $Co_3[Co(CN)_6]_2$.[6i] The maximum uptakes correspond to 2.0, 1.4 and 1.2 H_2 molecules per formula unit for ZnCr, MnCr and FeCr, respectively. For ZnCr, this gives a minimum volumetric H_2 storage density of 0.023 $Kg\,L^{-1}$, compared to 0.016–0.019 $Kg\,L^{-1}$ for $A_2Zn_3[Fe(CN)_6]_2$ (A = H, Li, Na, K, Rb)[6e] and 0.016–0.025 $Kg\,L^{-1}$ for $M_3[Co(CN)_6]_2$ (M = Mn, Fe, Co, Ni, Cu, Zn)[6i] under the same conditions. Although the value is relatively lower than some reported porous MOFs with much higher volumetric H_2 storage,[15] this material is still a potential viable hydrogen storage media for future mobile applications.

The measured temperature is well above the critical one (33 K) for hydrogen, which suggests that maximal sorption quantities at 860 Torr do not represent saturation loadings without much higher pressures. Adsorption isotherms were fitted by employing the Langmuir–Freundlich (L-F) equation,[16] which yielded estimated limiting sorption capacities of 1.66 wt.-% for ZnCr, 1.25 wt.-% for MnCr and 1.00 wt.-% for FeCr, compared to the highest predicted saturation capacity of 2.3 wt.-% in $Cu_2[Fe(CN)_6]$[6f] for any measured Prussian Blue analogues. A moderate H_2 uptake for FeCr with just 289 $m^2\,g^{-1}$ BET surface area may arise from the utility of the guest K^+ alkali metal cation for enhancing the H_2 binding affinity within the porous framework. The role of the alkali metal sited within the pore for the hydrogen adsorption has also been explored in alkali metal exchanged porous coordination polymers $A_2Zn_3[Fe(CN)_6]_2 \cdot xH_2O$[6d,6e] and zeolites.[17]

Conclusions

In summary, three porous Prussian blue analogues constructed from the $[Cr(CN)_6]^{3-}$ building block have been synthesized and structurally characterized. Hydrogen sorption studies demonstrated that guest the K^+ alkali metal cation located in the pores can perhaps enhance the H_2 binding affinity within the dehydrated porous framework. Future work will focus on performing H_2 adsorption isotherms at 87 K to quantify the strength between H_2 and the porous framework, doping with electropositive elements (such as, Li, Na, Rb, and maybe Cu, Ag and Au) to increase H_2 binding energy and varying the covalent metal types to exploit new materials for H_2 storage.

Experimental Section

Materials: Unless otherwise noted, all reactants were used as purchased, without further purification. $K_3[Cr(CN)_6]\cdot H_2O$ was prepared according to a published procedure.[18]

$KZn[Cr(CN)_6]\cdot xH_2O$: The crystalline powder was prepared by the reaction of $K_3[Cr(CN)_6]\cdot H_2O$ (2.0 mmol) and $ZnSO_4\cdot 7H_2O$ (2.0 mmol) in aqueous solution. Yield: 31% on the basis of $ZnSO_4\cdot 7H_2O$. $KZnCr(CN)_6\cdot 7H_2O$ (439): calcd. C 16.43, H 3.22, Cr 11.85, K 8.91, N 19.16, Zn 14.91; found C 16.14, H 3.17, Cr 11.68, K 8.79, N 19.32, Zn 15.09. The amount of water molecules per formula unit based on elemental and ICP analysis data is in agreement with the results determined from TG analysis (Figure 3). The crystallinity was checked by X-ray powder diffraction as shown in Figure 2. Light-yellow, block-shaped single crystals were obtained by slow diffusion of aqueous solutions of $K_3[Cr(CN)_6]\cdot H_2O$ (0.05 mmol) and $ZnSO_4\cdot 7H_2O$ (0.05 mmol). $C_6H_2CrKN_6OZn$ (331): calcd. C 21.80, H 0.61, Cr 15.73, K 11.83, N 25.42, Zn 19.78; found C 21.71, H 0.65, K 11.79, Cr 15.82, N 24.49, Zn 19.95.

$KMn[Cr(CN)_6]\cdot xH_2O$: The crystalline powder was prepared by the reaction of $K_3[Cr(CN)_6]\cdot H_2O$ (2.0 mmol) and $MnCl_2\cdot 4H_2O$ (2.0 mmol) in aqueous solution. Yield: 33% on the basis of $MnCl_2\cdot 4H_2O$. $KMnCr(CN)_6\cdot 8H_2O$ (446): calcd. C 16.15, H 3.61, Cr 11.65, K 8.76, N 18.83, Mn 12.31; found C 15.97, H 3.50, Cr 11.34, K 8.99, N 18.64, Mn 12.06. The amount of water molecules per formula unit based on elemental and ICP analysis data is in agreement with the results determined from TG analysis (Figure 3). The crystallinity was checked by X-ray powder diffraction as shown in Figure 2. Light-green, block-shaped single crystals were obtained by slow diffusion of aqueous solutions of $K_3[Cr(CN)_6]\cdot H_2O$ (0.05 mmol) and $MnCl_2\cdot 4H_2O$ (0.05 mmol). $C_6H_2CrKMnN_6O$ (320): calcd. C 22.51, H 0.63, Cr 16.24, K 12.21, Mn 17.16, N 26.25; found C 22.39, H 0.68, Cr 16.27, K 12.30, Mn 17.08, N 26.18.

$KFe[Cr(CN)_6]\cdot xH_2O$: The crystalline powder was prepared by the reaction of $K_3[Cr(CN)_6]\cdot H_2O$ (2.0 mmol) and $FeSO_4\cdot 5H_2O$ (2.0 mmol) in aqueous solution. Yield: 25% on the basis of $FeSO_4\cdot 5H_2O$. $KFeCr(CN)_6\cdot 6H_2O$ (411): calcd. C 17.53, H 2.94, Cr 12.65, Fe 13.58, K 9.51, N 20.44, found C 17.24, H 2.84, Cr 12.74, Fe 13.45, K 9.67, N 20.51. The amount of water molecules per formula unit based on elemental and ICP analysis data is in agreement with the results determined from TG analysis (Figure 3). The crystallinity was checked by X-ray powder diffraction as shown in Figure 2. Brick-red, block-shaped single crystals were obtained by slow diffusion of aqueous solutions of $K_3[Cr(CN)_6]\cdot H_2O$ (0.05 mmol) and $FeSO_4\cdot 5H_2O$ (0.05 mmol). $C_6H_2CrFeKN_6O$ (321): calcd. C 22.45, H 0.63, Cr 16.20, Fe 17.39, K 12.18, N 26.18; found C 22.38, H 0.70, Cr 16.13, Fe 17.48, K 12.01, N 26.21.

X-ray Crystallographic Analysis: Diffraction data for $MCr\cdot H_2O$ were collected with a Bruker Smart Apex diffractometer equipped with Mo-K_α (λ = 0.71073 Å) radiation (Table 3). Diffraction data analysis and reduction were performed within SMART, SAINT and XPREP.[19] Correction for Lorentz, polarization and absorption effects were performed within SADABS.[20] Structures were solved by using the patterson method within SHELXS-97[21] and refined by using SHELXL-97.[22] K and O atoms were fixed to have 50% occupancy each in the structure of $MCr\cdot H_2O$. CCDC-745564 (for FeCr), -729603 (for MnCr) and -729604 (ZnCr) contain the supplementary crystallographic data for this paper. These data can be obtained free of charge from The Cambridge Crystallographic Data Centre via www.ccdc.cam.ac.uk/data_request/cif.

Table 3. Crystallographic data and refinement details for $MCr\cdot H_2O$.

Compound	$ZnCr\cdot H_2O$	$MnCr\cdot H_2O$	$FeCr\cdot H_2O$
Chemical formula	$C_6H_2CrKN_6OZn$	$C_6H_2CrKN_6OMn$	$C_6H_2CrKN_6OFe$
Formula weight	330.61	320.18	321.09
Crystal system	cubic	cubic	cubic
Space group	$Fm\bar{3}n$	$Fm\bar{3}n$	$Fm\bar{3}n$
T / K	291(2)	291(2)	291(2)
a / Å	10.5801(7)	10.7936(11)	10.604(1)
V / Å^3	1184.32(14)	1257.5(2)	1192.37(19)
Z	4	4	4
$D_{calcd.}$ / g cm^{-3}	1.854	1.691	1.789
μ / mm^{-1}	3.280	2.185	2.462
GOF on F^2	1.051	1.004	1.047
R_1[a] [$I > 2\sigma(I)$]	0.0284	0.0182	0.0310
ωR_2[b] (all data)	0.0715	0.0532	0.1062

[a] $R_1 = \Sigma||F_o| - |F_c||/\Sigma|F_o|$. [b] $\omega R_2 = [\Sigma\omega(F_o^2 - F_c^2)^2/\Sigma\omega(F_o^2)^2]^{1/2}$.

Physical Measurements: Elemental analyses for C, H and N were performed with a Perkin–Elmer model 2400 CHN analyzer, whereas those for K, Cr and M (M = Zn, Mn, Fe) were determined by inductively coupled plasma (ICP) analysis by using a JY38S spectrometer. IR spectra were measured with a Nicolet FT 1703X spectrophotometer in the form of KBr pellets in the 4000–400 cm^{-1} region. Variable-temperature powder X-ray diffraction (XRD) patterns were collected with Cu-K_α radiation by using a D8-Advance X-ray diffractometer (Bruker-AXS). All the patterns were collected from 5 to 50°/2θ with a rate of 2° min^{-1}. Thermal gravimetric analyses (TGA) were carried out at a ramp rate of 2 °C min^{-1} under a dry nitrogen atmosphere by using a Perkin–Elmer Pyris Diamond TGA analyzer.

Gas Adsorption Measurements: Sample tubes of a known weight were loaded and sealed by using a transeal. Samples were degassed at 120 °C for 12 h with a Micromeritics ASAP 2020 analyzer until the outgas rate was no more than 1 mTorr min^{-1}. The degassed sample and sample tube were weighed and then transferred back to the analyzer (with the transeal preventing exposure of the sample to air after degassing). The outgas rate was again confirmed to be less than 1 mTorr min^{-1}. Samples were maintained at constant temperature by immersion in a liquid-nitrogen bath (77 K). UHP grade N_2 and H_2 (99.999%) gases were used for all measurements.

Supporting Information (see footnote on the first page of this article): IR spectra (ν_{CN} vibration region) of the as-synthesized samples and the samples after gas sorption experiments for MCr (M = Zn, Mn and Fe); variable-temperature powder XRD patterns of as-synthesized MnCr and FeCr.

Acknowledgments

The work is supported by the University Natural Science Foundation of Jiangsu Province (No. 07KJB150030, China).

[1] DOE Office of Energy Efficiency and Renewable Energy Hydrogen, Fuel Cells & Infrastructure Technologies Program Multi-Year Research, Development and Demonstration Plan, available at: http://www.eere.energy.gov/hydrogenandfuelcells/mypp.

[2] a) F. U. Naab, M. Dhoubhadel, J. R. Gilbert, M. C. Gilbert, L. K. Savage, O. W. Holland, J. L. Duggan, F. D. McDaniel, *Phys. Lett. A* **2006**, *356*, 152–155; b) S. K. Bhatia, A. L. Myers, *Langmuir* **2006**, *22*, 1688–1700.

[3] a) A. Zecchina, S. Bordiga, J. G. Vitillo, G. Ricchiardi, C. Lamberti, G. Spoto, M. Bjorgen, K. P. Lilleruk, *J. Am. Chem. Soc.* **2005**, *127*, 6361–6366; b) V. B. Kazansky, V. Y. Borovkov, A. Serich, H. G. Karge, *Microporous Mesoporous Mater.* **1998**, *22*, 251–259.

[4] a) X. Lin, I. Telepeni, A. J. Blake, A. Dailly, C. M. Brown, J. M. Simmons, M. Zoppi, G. S. Walker, K. M. Thomas, T. J. Mays, P. Hubberstey, N. R. Champness, M. Schroder, *J. Am. Chem. Soc.* **2009**, *131*, 2159–2171; b) X. S. Wang, S. Q. Ma, P. M. Forster, D. Q. Yuan, J. Eckert, J. J. Lopez, B. J. Murphy, J. B. Parise, H. C. Zhou, *Angew. Chem. Int. Ed.* **2008**, *47*, 7263–7266; c) M. Dincă, J. R. Long, *Angew. Chem. Int. Ed.* **2008**, *47*, 6766–6779; d) S. S. Han, W. Q. Deng, W. A. Goddard, *Angew. Chem. Int. Ed.* **2007**, *46*, 6289–6292; e) X. B. Zhao, B. Xiao, A. J. Fletcher, K. M. Thomas, D. Bradshaw, M. J. Rosseinsky, *Science* **2004**, *306*, 1012–1015; f) S. Kitagawa, R. Kitaura, S. Noro, *Angew. Chem. Int. Ed.* **2004**, *43*, 2334–2375; g) N. L. Rosi, J. Eckert, M. Eddaoudi, D. T. Vodak, J. Kim, M. O'Keeffe, O. M. Yaghi, *Science* **2003**, *300*, 1127–1129.

[5] a) J. N. Behera, D. M. D'Alessandro, N. Soheilnia, J. R. Long, *Chem. Mater.* **2009**, *21*, 1922–1926; b) C. P. Krap, B. Zamora, L. Reguera, E. Reguera, *Microporous Mesoporous Mater.* **2009**,

120, 414–420; c) S. S. Kaye, H. J. Choi, J. R. Long, *J. Am. Chem. Soc.* **2008**, *130*, 16921–16925; d) J. T. Culp, M. R. Smith, E. Bittner, B. Bockrath, *J. Am. Chem. Soc.* **2008**, *130*, 12427–12434; e) J. T. Culp, S. Natesakhawat, M. R. Smith, E. Bittner, C. Matranga, B. Bockrath, *J. Phys. Chem. C* **2008**, *112*, 7079–7083; f) C. X. Chu, A. H. Yuan, W. Y. Liu, X. Q. Shen, X. F. Meng, *Acta Chim. Sinica* **2008**, *24*, 2700–2704; g) M. Avila, L. Reguera, J. Rodríguez-Hernández, J. Balmaseda, E. Reguera, *J. Solid State Chem.* **2008**, *181*, 2899–2907; h) Y. Li, Y. Liu, Y. T. Wang, Y. H. Leng, L. Xie, X. G. Li, *Int. J. Hydrogen Energ.* **2007**, *32*, 3411–3415; i) J. Roque, E. Reguera, J. Balmaseda, J. Rodríguez-Hernández, L. Reguera, L. F. del Castillo, *Microporous Mesoporous Mater.* **2007**, *103*, 57–71; j) J. Balmaseda, E. Reguera, J. Rodríguez-Hernández, L. Reguera, M. Autie, *Microporous Mesoporous Mater.* **2006**, *96*, 222–236; k) E. Reguera, J. Balmaseda, J. Rodríguez-Hernández, *J. Porous Mater.* **2004**, *11*, 219–228; l) J. Balmaseda, E. Reguera, A. Gomez, J. Roque, C. Vazquez, M. Autie, *J. Phys. Chem. B* **2003**, *107*, 11360–11369.

[6] a) L. Reguera, J. Balmaseda, C. P. Krap, E. Reguera, *J. Phys. Chem. C* **2008**, *112*, 17443–17449; b) L. Reguera, C. P. Krap, J. Balmaseda, E. Reguera, *J. Phys. Chem. C* **2008**, *112*, 15893–15899; c) L. Reguera, J. Balmaseda, C. P. Krap, E. Reguera, *J. Phys. Chem. C* **2008**, *112*, 10490–10501; d) L. Reguera, J. Balmaseda, L. F. del Castillo, E. Reguera, *J. Phys. Chem. C* **2008**, *112*, 5589–5597; e) S. S. Kaye, J. R. Long, *Chem. Commun.* **2007**, 4486–4488; f) S. S. Kaye, J. R. Long, *Catal. Today* **2007**, *120*, 311–316; g) S. Natesakhawat, J. T. Culp, C. Matranga, B. Bockrath, *J. Phys. Chem. C* **2007**, *111*, 1055–1060; h) J. T. Culp, C. Matranga, M. Smith, E. W. Bittner, B. Bockrath, *J. Phys. Chem. B* **2006**, *110*, 8325–8328; i) S. S. Kaye, J. R. Long, *J. Am. Chem. Soc.* **2005**, *127*, 6506–6507; j) K. W. Chapman, P. D. Southon, C. L. Weeks, C. J. Kepert, *Chem. Commun.* **2005**, 3322–3324.

[7] M. R. Hartman, V. K. Peterson, Y. Liu, *Chem. Mater.* **2006**, *18*, 3221–3224.

[8] M. Avila, L. Reguera, C. Vargas, E. Reguera, *J. Phys. Chem. Solids* **2009**, *70*, 477–482.

[9] a) Z. L. Lü, X. Y. Wang, Z. L. Liu, F. H. Liao, S. Gao, R. G. Xiong, H. W. Ma, D. Q. Zhang, D. B. Zhu, *Inorg. Chem.* **2006**, *45*, 999–1004; b) H. U. Güdel, H. Stucki, A. Lüdi, *Inorg. Chim. Acta* **1973**, *7*, 121–124; c) G. Ron, A. Lüdi, P. Engel, *Chimia* **1973**, *27*, 77–79; d) H. U. Güdel, *Acta Chem. Scand.* **1972**, *26*, 2169; e) A. Lüdi, H. U. Güdel, M. Rüegg, *Inorg. Chem.* **1970**, *9*, 2224–2227.

[10] A. L. Spek, *J. Appl. Crystallogr.* **2003**, *36*, 7–13.

[11] a) G. W. Beall, W. O. Milligan, J. Kopp, I. Bernal, *Inorg. Chem.* **1977**, *16*, 2715–2718; b) F. Herren, P. Fischer, A. Ludi, W. Halg, *Inorg. Chem.* **1980**, *19*, 956–959.

[12] J. Rodriguez-Carvajal, *Physica B* **1993**, *192*, 55–69.

[13] F. Rouquerol, J. Rouquerol, K. S. W. Sing, *Absorption by Powders and Porous Solids: Principles, Methodology and Applications*, Academic Press, San Diego, London, **1999**.

[14] B. L. Chen, N. W. Ockwig, A. R. Millward, D. S. Contreras, O. M. Yaghi, *Angew. Chem. Int. Ed.* **2005**, *44*, 4745–4749.

[15] a) H. Chun, H. Jung, G. Koo, H. Jeong, D. K. Kim, *Inorg. Chem.* **2008**, *47*, 5355–5359; b) J. L. Belof, A. C. Stern, M. Eddaoudi, B. Space, *J. Am. Chem. Soc.* **2007**, *129*, 15202–15210; c) X. Lin, J. H. Jia, X. B. Zhao, K. M. Thomas, A. J. Blake, G. S. Walker, N. R. Champness, P. Hubberstey, M. Schröder, *Angew. Chem. Int. Ed.* **2006**, *45*, 7358–7364; d) P. Krawiec, M. Kramer, M. Sabo, R. Kunschke, H. Fröde, S. Kaskel, *Adv. Eng. Mater.* **2006**, *8*, 293–296; e) L. Pan, B. Parker, X. Y. Huang, D. H. Olson, J. Lee, J. Li, *J. Am. Chem. Soc.* **2006**, *128*, 4180–4181.

[16] R. T. Yang, *Gas Separation by Adsorption Processes*, Butterworth, Boston, MA, **1987**.

[17] a) F. J. Torres, J. G. Vitillo, B. Civalleri, G. Ricchiardi, A. Zecchina, *J. Phys. Chem. C* **2007**, *111*, 2505–2513; b) F. J. Torres, B. Civalleri, A. Terentyev, P. Ugliengo, C. Pisani, *J. Phys. Chem. C* **2007**, *111*, 1871–1873; c) G. T. Palomino, M. R. L. Carayol, C. O. Areán, *J. Mater. Chem.* **2006**, *16*, 2884–2885.

[18] V. Marvaud, T. Mallah, M. Verdaguer, M. Biner, S. Decurtins, *Inorg. Synth.* **2004**, *34*, 144–146.

[19] Bruker, *SMART*, *SAINT* and *XPREP*: *Area Detector Control and Data Integration and Reduction Software*, Bruker Analytical X-ray Instruments Inc., Madison, Wisconsin, US, **1995**.

[20] G. M. Sheldrick, *SADABS*: *Empirical Absorption and Correction Software*, University of Göttingen, Göttingen, Germany, **1999**.

[21] G. M. Sheldrick, *SHELXS-97*: *Programs for Crystal Structure Solution*, University of Göttingen, Göttingen, Germany, **1997**.

[22] G. M. Sheldrick, *SHELXL-97*: *Programs for the Refinement of Crystal Structures*, University of Göttingen, Göttingen, Germany, **1997**.

Received: September 11, 2009
Published Online: January 8, 2010

